

Reductive Electrochemistry of Rhodium Porphyrins. Disproportionation of Intermediary Oxidation States

Valérie Grass,^{1a} Doris Lexa,^{1a,b} Michel Momenteau,^{1c} and Jean-Michel Savéant^{*,1a}

Contribution from the Laboratoire d'Electrochimie Moléculaire de l'Université Denis Diderot, Unité Associée au CNRS No 438, 2 place Jussieu, 75251 Paris Cedex 05, and the Institut Curie, Unité Inserm 219, Orsay 91405, France

Received November 20, 1996[®]

Abstract: The reduction of rhodium(III) porphyrins in polar aprotic solvents is a two-electron irreversible reaction yielding directly the Rh(I) complex. The cause of this irreversibility is not the metal–metal dimerization of the initially formed Rh(II) complex as believed earlier but rather deligation which generates a secondary Rh(II) species easier to reduce than the starting Rh(III) porphyrin. This is confirmed by the fact that sterically encumbered porphyrins, such as those bearing cross-trans basket-handle superstructures which forbid the approach of two molecules at bonding distance, exhibit the same behavior as simple rhodium porphyrins. The occurrence of such an ECE–disproportionation process, seldom observed in the redox chemistry of metallo-porphyrins or similar complexes, is probably related to the tendency of the rhodium atom to shift out of the porphyrin plane, particularly at the Rh(I) oxidation state. It is remarkable that strong and soft ligands, e.g., tertiary phosphines, annihilate the disproportionation of the rhodium(II) complex.

Metalloporphyrins have been often used as homogeneous catalysts of electrochemical reactions, particularly reductions. The principle of this catalytic process consists in the electrochemical generation of a low-valent form of the metalloporphyrin which converts the substrate into the desired product while regenerating the starting metalloporphyrin thus triggering a new catalytic cycle. Although low-valent metalloporphyrins may be generated by a simple outersphere single electron transfer from the electrode, it is expected that they will not themselves react with the substrate as outersphere electron donors but rather that they will integrate transiently the substrate into their coordination sphere. These chemical catalytic processes, involving innersphere pathways, are indeed expected to be more efficient, both in terms of rate and selectivity, than redox catalytic processes in which catalysis has a physical origin, namely, the electron donor is dispersed three-dimensionally instead of being confined on a surface as in the direct electrochemical reaction.²

The main reactions where low-valent metalloporphyrins have been used as catalysts are reductions of small molecules such as dioxygen,³ carbon dioxide,⁴ NO, NO₂, and NO₃²⁻.⁵ Chemical rather than redox catalysis is deemed to occur in these reactions.

Hydrogen evolution from acids has also been shown to be catalyzed by low-valent porphyrins of cobalt,⁶ ruthenium,⁷ and iron.^{8a}

Since rhodium porphyrin hydrides (Rh(III)H) have been obtained by chemical reduction of rhodium(III) porphyrins and protonation of the rhodium(I) porphyrins thus produced, it would seem interesting to try rhodium porphyrins as chemical catalysts for electrochemical hydrogen evolution or hydrogenation. One may indeed envision an electrochemical reaction where the rhodium(III) porphyrin would be reduced at the rhodium(I) stage. The latter complex would then be converted into the rhodium(III) hydride by an acid added to the solution, and the H⁻ donor properties of this hydride or its reduced form, Rh(II)H⁻, would be exploited in hydrogen evolution or hydrogenation reactions.^{8b}

A first necessary step in this direction involves in examining how rhodium(III) porphyrins may be electrochemically converted into the corresponding rhodium(I) porphyrins. One problem in this connection is the instability of rhodium(II) porphyrins, which appears to complicate the reductive electrochemistry of rhodium(III) porphyrins. One source of irrevers-

[®] Abstract published in *Advance ACS Abstracts*, April 1, 1997.

(1) (a) Université Denis Diderot. (b) Permanent address: Laboratoire de Bioénergétique and Ingénierie des Protéines, UPR CNRS 9036, 31 Chemin J. Aiguier, 13009 Marseille, France. (c) Institut Curie.

(2) (a) Andrieux, C. P.; Dumas-Bouchiat, J.-M.; Savéant, J.-M. *J. Electroanal. Chem.* **1978**, *87*, 39. (b) Andrieux, C. P.; Savéant, J.-M. *Electrochemical Reactions In Investigations of Rates and Mechanisms*; Bernasconi, C. F., Ed.; Wiley: New York, 1986; Vol. 6, 4/E, Part 2, p 305.

(3) (a) Collman, J. P.; Marroco, M.; Denisevich, P.; Koval, C.; Anson, F. C. *J. Electroanal. Chem. Interfacial Electrochem.* **1979**, *101*, 117. (b) Chang, C. K.; Liu, H. Y.; Abdalmuhdi, I. *J. Am. Chem. Soc.* **1984**, *106*, 2725. (c) Collman, J. P.; Wagenknecht, P. S.; Hutchison, J. E. *Angew. Chem., Int. Ed. Engl.* **1994**, *33*, 1537. (d) Shi, C.; Anson, F. C. *J. Am. Chem. Soc.* **1991**, *113*, 9564. (e) Shi, C.; Anson, F. C. *Inorg. Chem.* **1992**, *31*, 5078. (f) Steiger, B.; Anson, F. C. *Inorg. Chem.* **1995**, *34*, 3355. (g) Shi, C.; Anson, F. C. *Inorg. Chem.* **1995**, *34*, 4554.

(4) (a) Hammouche, M.; Lexa, D.; Savéant, J.-M. *J. Am. Chem. Soc.* **1987**, *113*, 8455. (b) Bhugun, I.; Lexa, D.; Savéant, J.-M. *J. Am. Chem. Soc.* **1994**, *116*, 5015. (c) Bhugun, I.; Lexa, D.; Savéant, J.-M. *J. Am. Chem. Soc.* **1996**, *118*, 1769. (d) Bhugun, I.; Lexa, D.; Savéant, J.-M. Submitted.

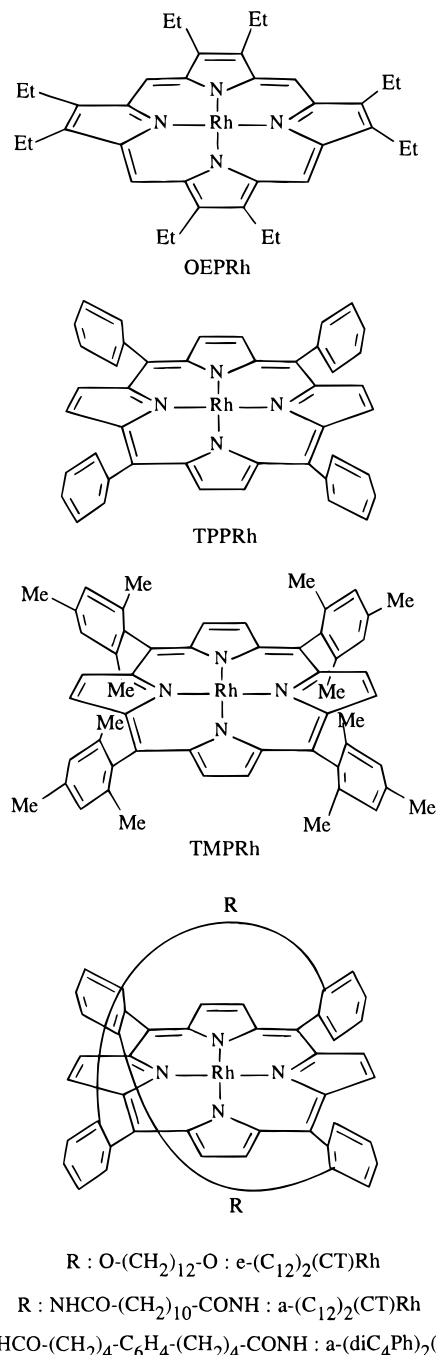
(5) (a) Choi, I.; Ryan, M. *New J. Chem.* **1992**, *16*, 591. (b) Kyu Choi, I.; Liu, Y.; Feng, D.; Paeng, K.; Ryan, M. *Inorg. Chem.* **1991**, *30*, 1832. (c) Fernandez, J.; Feng, D.; Chang, A.; Keyser, A.; Ryan, M. *Inorg. Chem.* **1986**, *25*, 2606. (d) Feng, D.; Ting, Y.; Ryan, M. *Inorg. Chem.* **1985**, *24*, 612. (e) Choi, I.; Ryan, M. *Chim. Acta* **1988**, *153*, 25. (f) Barley, M.; Takeuchi, K.; Murphy, W.; Meyer, T. J. *Chem. Soc., Chem. Commun.* **1985**, 507. (g) Barley, M.; Takeuchi, K.; Meyer, T. J. *Am. Chem. Soc.* **1986**, *108*, 5876.

(6) (a) Connolly, P.; Espenson, J. H. *Inorg. Chem.* **1986**, *25*, 2684. (b) Kellett, R. M.; Spiro, T. G. *Inorg. Chem.* **1985**, *24*, 2378. (c) Kellett, R. M.; Spiro, T. G. *Inorg. Chem.* **1985**, *24*, 2373.

(7) (a) Collman, J. P.; Ha, Y.; Guilard, R.; Lopez, M.-A. *Inorg. Chem.* **1993**, *32*, 1788. (b) Collman, J. P.; Wagenknecht, P. S.; Hembre, R. T.; Lewis, N. S. *J. Am. Chem. Soc.* **1990**, *112*, 1294. (c) Collman, J. P.; Wagenknecht, P. S.; Hutchison, J. E.; Lewis, N. S.; Guilard, R.; Lopez, M.-A.; L'Her, M.; Bothner-By, A. A.; Mishra, P. K. *J. Am. Chem. Soc.* **1992**, *114*, 5654. (d) Collman, J. P.; Ha, Y.; Guilard, R.; Lopez, M.-A.; Wagenknecht, P. S. *J. Am. Chem. Soc.* **1993**, *115*, 9080. (e) Collman, J. P.; Wagenknecht, P. S.; Hutchison, J. E. *Angew. Chem., Int. Ed. Engl.* **1994**, *33*, 1537. (f) Collman, J. P.; Wagenknecht, P. S.; Hutchison, J. E. *J. Am. Chem. Soc.* **1992**, *114*, 5665.

(8) (a) Bhugun, I.; Lexa, D.; Savéant, J.-M. *J. Am. Chem. Soc.* **1996**, *118*, 3982. (b) Grass, V.; Lexa, D.; Savéant, J.-M. Submitted.

Chart 1



ibility is metal-metal dimerization of two rhodium(II) complexes as observed in apolar solvents with rhodium(II) porphyrins generated by photolysis of TPPRh-CH₃^{9a} (TPP: see Chart 1) or TPP(Rh(I))₂(CO)₄.¹⁰ The formation of the dimer is prevented by steric hindrance as in the case where TPP is replaced by tetramesitylporphyrin.⁹ The irreversibility of the cyclic voltammetric reduction wave of TPPRh(III) observed in polar aprotic solvents (benzonitrile, tetrahydrofuran, pyridine) has been attributed to dimerization of the rhodium(II) complex,¹¹ whereas dimerization does not seem to interfere in the reduction of

(9) (a) Wayland, B. B.; Ba, S.; Sherry, A. E. *J. Am. Chem. Soc.* **1991**, *113*, 5305. (b) Sherry, A. E.; Wayland, B. B. *J. Am. Chem. Soc.* **1990**, *112*, 1259. (c) Sherry, A. E.; Wayland, B. B.; Poszmiak, G.; Bunn, A. G. *J. Am. Chem. Soc.* **1992**, *114*, 1673. (d) Wayland, B. B.; Balkus, K. J.; Farnos, M. D. *Organometallics* **1989**, *8*, 950.

(10) Yamamoto, S.; Hoshino, M.; Yasufuku, K.; Imamura, M. *Inorg. Chem.* **1984**, *23*, 195.

(11) (a) Kadish, K. M.; Yao, C.-L.; Anderson, J. E.; Cocolios, P. *Inorg. Chem.* **1985**, *24*, 4515. (b) Kadish, K. M.; Hu, Y.; Boschi, T.; Tagliatesta, P. *Inorg. Chem.* **1993**, *32*, 2996.

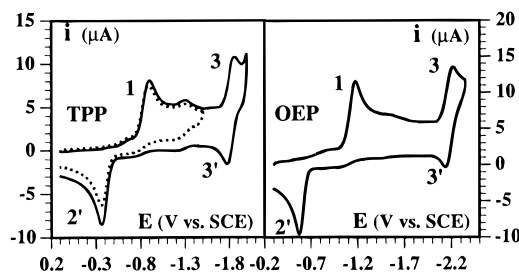


Figure 1. Cyclic voltammetry of TPPRh (1 mM) and OEPRhCl (1 mM) in DMSO + 0.1 M Et₄NClO₄. Scan rate: 0.1 V/s. Temperature: 20 °C.

rhodium(III) tetramesitylporphyrin in a weakly polar solvent (1,2-difluorobenzene).¹²

As reported below, we have found that the cause of the chemical irreversibility of the electrochemical reduction of rhodium(III) porphyrins is not the dimerization of the rhodium(II) complexes but rather their disproportionation triggered by ligand exchange reactions. This will be demonstrated using the simple TPP and OEP porphyrins and also the basket-handle porphyrins shown in the chart.

Disproportionation of intermediary oxidation states has been rarely observed in the redox chemistry of metalloporphyrins or related complexes such as B12 derivatives. For example, iron porphyrins give rise to chemically reversible successive redox couples (Fe(III)/Fe(II)/Fe(I)/Fe(0)).¹³ Cobalt(II) corrins and porphyrins exhibit some tendency to disproportionate only when they bear cyanide ions as axial ligands.¹⁴

Results and Discussion

Simple Porphyrins. Figure 1 shows typical examples of the cyclic voltammetry of unencumbered rhodium(III) porphyrins. Similar voltammograms are obtained in dimethylsulfoxide (DMSO), dimethylformamide (DMF), and butyronitrile (Table 1). The first cathodic wave (1), whose height seems to correspond to a two-electron reduction, leads to a product that is oxidized (wave 2'), after the exchange of also two electrons, at a significantly more positive potential. The numbering of the waves, 1 for the first cathodic wave and 2' for the reoxidation of the product formed at the first wave, derives from the fact that these two waves do not represent the reactions of the two members of a one-electron reversible couple. A reversible one-electron wave, 3/3', is observed at a much more negative potential. The peak potential characteristics of the various rhodium(III) porphyrins in various solvents are summarized in Table 1.

Coulometry during reductive preparative-scale electrolysis at a potential located just beyond the peak potential of wave 1 shows that two electrons are consumed thus pointing to the direct formation of the rhodium(I) porphyrin from the rhodium(III) porphyrin (Table 2).

Another way of showing that the rhodium(I) porphyrin is indeed formed at the cathodic wave 1 is to carry out a preparative-scale electrolysis at a potential just beyond the wave and examine the electrolyzed solution by means of cyclic voltammetry. This is shown in Figure 2 for the reduction of TPPRh(III)Cl in DMF. After electrolysis at -1.1 V vs SCE, the potential is scanned from this value toward the positive

(12) Vitols, S. E.; Friesen, D. A.; Williams, D. S.; Melamed, D.; Spiro, T. G. *J. Phys. Chem.* **1996**, *100*, 207.

(13) Gueutin, C.; Lexa, D.; Momenteau, M.; Savéant, J.-M.; Xu, F. *Inorg. Chem.* **1986**, *25*, 4294.

(14) (a) Lexa, D.; Savéant, J.-M.; Zickler, J. *J. Am. Chem. Soc.* **1980**, *102*, 2654. (b) Amatore, C.; Lexa, D.; Savéant, J.-M. *J. Electroanal. Chem.* **1980**, *111*, 81. (c) Lexa, D.; Lhoste, J.-M. *Experientia Suppl.* **1971**, *18*, 395.

Table 1. Cyclic Voltammetry of Rhodium(III) Porphyrins and Peak Potentials^a

solvent	compound	1	1'	2	2'	3	3'
DMSO ^b	TPPRhI	-0.90			-0.35	-1.86	-1.80 (-1.83, 60)
	TPPRhCl	-0.97			-0.37	-1.89	-1.83 (-1.86, 60)
	OEPRhCl	-1.18			-0.57	-2.21	-2.14 (-2.17, 70)
<i>n</i> -PrCN ^c	TPPRhI	-1.23			-0.26	-2.00	-1.93 (-1.96, 70)
	+0.05 M PEt ₃	-1.07	-1.00	-1.78	-1.71		
	+0.1 M PCH ₃ Ph ₂	-1.12	-1.05	-1.57			
	+0.2 M PPh ₃	-0.89			-0.44	-2.03	-1.96 (-1.99, 70)
DMF ^b	TPPRhI	-1.09			-0.16	-1.89	-1.82 (-1.85, 70)
	TPPRhCl	-1.02			-0.14	-1.84	-1.78 (-1.81, 60)
	TPPRhNH(CH ₃) ₂ Cl	-1.16			-0.13	-1.85	-1.78 (-1.82, 70)
	a-(diC ₄ Ph) ₂ (CT)RhCl	-1.08			-0.14	-1.86	-1.80 (-1.83, 60)
	a-(C ₁₂) ₂ (CT)RhCl	-1.03			-0.25	-1.85	-1.78 (-1.81, 70)
	e-(C ₁₂) ₂ (CT)RhCl	-1.34			-0.40	-2.10	-2.04 (-2.07, 60)

^a In V vs SCE, scan rate: 0.1 V/s. Temperature: 20 °C. Between parentheses, for reversible waves, standard potential in V vs SCE and cathodic-to-anodic peak potential difference (in mV) successively. ^b +0.1 M Et₄NClO₄. ^c +0.1 M *n*-Bu₄NClO₄.

Table 2. Coulometry of the Reduction and Reoxidation of Rhodium(III) Porphyrins

solvent	compound	<i>n</i> _{red}	<i>n</i> _{reox}
DMSO	TPPRhI	2.0	1.7
	TPPRhCl	1.8	1.6
<i>n</i> -PrCN	TPPRhI	2.0	2.0
DMF	TPPRhCl	1.9	1.6
	TPPRhNH(CH ₃) ₂ Cl	2.0	2.1

direction showing a two-electron irreversible wave which corresponds to the reoxidation of the Rh(I) complex into a Rh(III) complex (Figure 2b). If the potential is scanned in the reverse direction, the one-electron reversible wave 3/3' only appears (Figure 2b). When the electrolyzed solution is re-oxidized at 0.0 V vs SCE, i.e., beyond the anodic wave 2', the cyclic voltammogram of the resulting solution (Figure 2c) is identical to the voltammogram of the initial solution (Figure 2a). Coulometry during this re-oxidizing electrolysis indicates again the exchange of two electrons per molecule (Table 2).

The conversion of the Rh(III) porphyrin into the Rh(I) porphyrin can also be followed by thin-layer spectroelectrochemistry, as represented in Figure 3 for TPPRhI in DMSO. The final spectrum thus obtained is identical to the spectrum obtained by reduction of the same compound with sodium borohydride which was previously assigned to the Rh(I) complex on the basis of ¹H NMR.^{15,16} It is also identical to the Rh(I) spectrum obtained in a recent pulse radiolysis study.¹⁷ The UV-vis spectral characteristics of the various initial Rh(III) porphyrins and those of their reduction product at wave 1 are summarized in Table 3. They are different from those of the Rh(II)-Rh(II) dimers which exhibit bands at 408 and 512 nm

(15) (a) Ogoshi, H.; Setsune, J.; Yoshida, Z. *J. Am. Chem. Soc.* **1977**, *99*, 3869. (b) Setsune, J.; Yoshida, Z.; Ogoshi, H. *J. Chem. Soc., Perkin Trans.* **1982**, 983.

(16) Wayland, B. B.; Van Vorhees, S. L.; Wilker, C. *Inorg. Chem.* **1986**, *25*, 4039.

(17) Grodkowski, J.; Neta, P.; Hambright, P. *J. Phys. Chem.* **1995**, *99*, 6019.

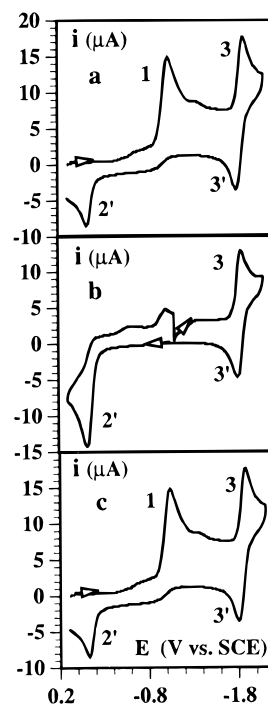


Figure 2. Cyclic voltammetry of TPPRhCl (1 mM) in DMF + 0.1 M Et₄NClO₄. Scan rate: 0.1 V/s. Temperature: 20 °C. (a) Before electrolysis. (b) After electrolysis at -1.1 V vs SCE. (c) after reoxidizing electrolysis at 0.0 V vs SCE.

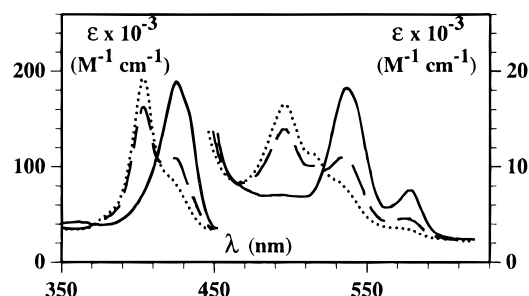


Figure 3. Thin-layer spectroelectrochemistry of TPPRhI (0.25 mM) in DMSO + 0.1 M Et₄NClO₄. Solid line: initial complex. Dotted line: after electrolysis at -1.0 V vs SCE. Dashed line: intermediary spectrum.

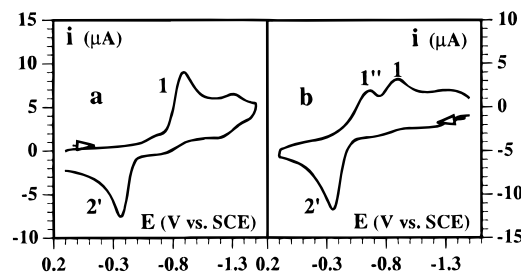


Figure 4. Cyclic voltammetry of TPPRhI (1 mM) in DMSO + 0.1 M Et₄NClO₄. Scan rate: 0.1 V/s. Temperature: 20 °C. Potential scan: (a) 0.0 → -1.5 → 0.0; (b) -1.5 → 0.0 → -1.5 V vs SCE.

for TPP.^{9a} The spectra of the reduction product are consistent with a Rh(I) complex where most of the electron density stands on the rhodium atom. This assignment is supported by the fact that rhodium-*o*-alkyl complexes and rhodium-hydrides are obtained upon reaction with alkyl halides and acids, respectively.^{8b,18}

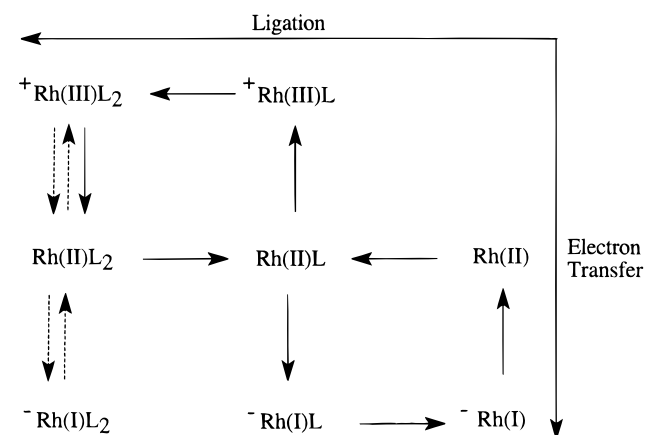
When the Rh(I) complex obtained upon reductive electrolysis in DMSO is re-oxidized at a potential just beyond the peak 2', a Rh(III) complex is regenerated. Its UV-vis bands are,

(18) Lexa, D.; Grass, V.; Savéant, J.-M., Manuscript in preparation.

Table 3. UV-vis Spectral Characteristics of Rhodium(III) Porphyrins and of Their Reduction Products

solvent	compound	oxidation state ^c	λ ($\epsilon \times 10^{-3}$) nm (L mol ⁻¹ cm ⁻¹)
DMSO ^a	TPPRhI	initial Rh(III)	426 (188) 538 (19.1) 578 (7.9)
		after reduction at -1.0 V	403 (192) 496 (16.5)
	TPPRhCl	initial Rh(III)	430 (239) 538 (18.2) 572 (5.6)
		after reduction at -1.1 V	406 (144) 496 (12.9)
	OEPRhCl	initial Rh(III)	408 (128) 520 (32.8) 552 (39.2)
		after reduction at -1.3 V	386 (142) 515 (46.4)
<i>n</i> -PrCN ^b	TPPRhI	initial Rh(III)	422 (200) 532 (16.2) 570 (5.9)
		after reduction at -1.3 V	400 (148) 493 (13.1)
	TPPRhI	initial Rh(III)	364 (60.7) 449 (150) 561 (8.1) 601 (11.5)
		after reduction at -1.2 V	472 (46.8) 538 (6.3) 730 (8.0) 782 (2.8) 885(8.1)
	TPPRhI	initial Rh(III)	406 (156) 499(12.5)
		after reduction at -1.8 V	449 (220) 558 (16.3) 598 (15.5)
DMF ^a	TPPRhI	initial Rh(III)	406 (238) 500 (18.9)
		after reduction at -1.0 V	406 (157) 498 (12.9)
	TPPRhCl	initial Rh(III)	422 (200) 534 (20.9) 574 (7.7)
		after reduction at -1.2 V	403 (198) 496 (17.9)
	TPPRhCl	initial Rh(III)	403 (112) 442 (52) 496 (13.7) 790 (14.0)
		after reduction at -2.0 V	421 (198) 533 (20.8) 568 (4.2)
TPPRhNH(CH ₃) ₂ Cl	initial Rh(III)	403 (194) 496 (15.4)	
	after reduction at -1.2 V	424 (235) 536 (22.4) 570 (5.9)	
DMF ^a	a-(diC ₄ Ph) ₂ (CT)RhCl	initial Rh(III)	403 (220) 496 (17.0)
		after reduction at -1.3 V	427 (212) 534 (21.8) 570 (3.7)
	a-(C ₁₂) ₂ (CT)RhCl	initial Rh(III)	404 (194) 498 (16.2)
		after reduction at -1.3 V	404 (247) 536 (13.5) 568 (2.5)
	e-(C ₁₂) ₂ (CT)RhCl	initial Rh(III)	404 (245) 499 (10.5)
		after reduction at -1.5 V	430 (153) 540 (14.9) 574 (3.2)
		after reduction at -1.5 V	408 (146) 505 (10.3)

^a +0.1 M Et₄NClO₄. ^b +0.1 M *n*-Bu₄NClO₄. ^c Reduction potential in V vs SCE.

Scheme 1

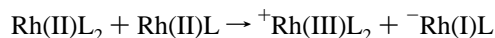
L : I⁻, Cl⁻, NH(CH₃)₂, solvent molecule (the indicated charges are for the case of a negatively charged ligand)

however, slightly different from those of the initial complex (423 (248), 532 (22.5), 566 (6.3)) for TPPRhI (to be compared with the first entry in Table 3). This observation points to the partial replacement of I⁻ by a DMSO molecule in the coordination sphere of Rh(III). This phenomenon can also be seen in cyclic voltammetry, as illustrated in Figure 4. When the scan is started toward negative potentials from a potential where the Rh(I) complex is generated at the electrode surface, the anodic wave 2' is first observed, and upon scan reversal, two rereduction waves, 1'' and 1, appear (Figure 4b) instead of one (Figure 4a).

All of the preceding observations can be rationalized in the framework of Scheme 1 which represents the coupling between the various possible electron transfer and ligand exchange reactions. Under the conditions investigated so far, the reduction and reoxidation pathways follow the solid arrows in Scheme 1.

During the reduction process (descending and left-to-right solid arrows), the initial Rh(III) complex is converted by means of a one-electron transfer into a Rh(II) complex bearing the same axial ligands. One of these is rapidly expelled leading to a

second Rh(II) complex which is easier to reduce than the initial Rh(III) complex. The Rh(I) complex thus formed may finally lose the remaining ligand. This is a classical "ECE" mechanism. These mechanisms are very common in organic electrochemistry^{2b} and have been observed in a few cases in coordination chemistry.^{14,19} The appearance of a two-electron process derives from the fact that the second Rh(II) complex can be reduced at the electrode surface more easily than the starting Rh(III) complex. This is what the second "E" of ECE stands for. It also follows that the following disproportionation of Rh(II) is a downhill reaction.



There is thus a "disproportionation" version of the ECE mechanism where the second electron transfer step takes place in the solution concurrently with the electrode reaction.^{2b,19}

During the reoxidation process (ascending and right-to-left solid arrows in Scheme 1), the final Rh(I) complex first transfers one electron to the electrode leading to a Rh(II) complex which undergoes a ligation reaction making it easier to oxidize than the Rh(I) complex. The reaction thus follows an "ECE-disproportionation" pathway in the reverse direction. However, as depicted in Scheme 1, the Rh(I) reoxidation pathway is not the exact reverse of the Rh(III) reduction pathway.²⁰

The reversible one-electron wave 3 that we found in all cases corresponds to the reversible reduction of the Rh(I) complex yielding presumably the anion radical by analogy with the "ring wave" observed with cobalt porphyrins in approximately the same potential region (see Figure 2a in ref 21). This is

(19) (a) Mastragostino, M.; Nadjio, L.; Savéant, J.-M. *Electrochim. Acta* **1968**, *13*, 721. (b) Mastragostino, M.; Savéant, J.-M. *Electrochim. Acta* **1968**, *13*, 751.

(20) At first sight, this may seem to contradict the principle of microscopic reversibility. In fact, the electrode electrons involved in the oxidation pathway "are not the same" as those involved in the reduction pathway (their energy is around -0.90 V vs SCE in the first case and around -0.35 V vs SCE in the second).

(21) Lexa, D.; Savéant, J.-M.; Soufflet, J.-P. *J. Electroanal. Chem.* **1979**, *100*, 159.

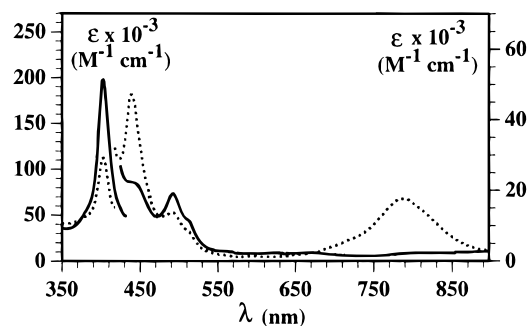


Figure 5. Thin-layer spectroelectrochemistry of TPPRh(I) (1 mM) in DMF + 0.1 M Et₄NClO₄. Solid line: Rh(I) complex obtained after electrolysis at -1.2 V vs SCE. Dotted line: after electrolysis at -2.0 V vs SCE.

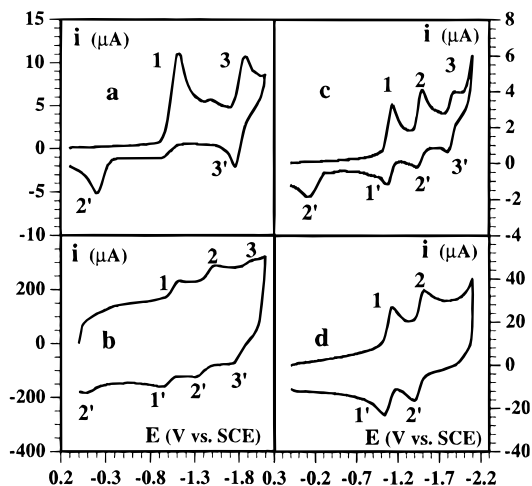


Figure 6. Cyclic voltammograms of *a*-(di-C₄Ph)₂(CT)Rh(III)Cl (1 mM) in DMF + 0.1 M Et₄NClO₄. Scan rate: 0.1 (a, c), 60 (b), 4 (d) V/s. Temperature: 20 °C (a, b), -20 °C (c, d).

confirmed by thin-layer spectroelectrochemistry at a potential just beyond the peak of wave 3. The resulting spectrum (Figure 5, Table 3) is similar to the spectrum obtained for the anion radical of zinc(II) TPP.²²

Basket-Handle Porphyrins. The steric hindrance created by the cross-trans basket-handle superstructures shown in the chart are expected to shut down the metal–metal dimerization of Rh(II) complexes, if this reaction were to interfere in the reduction of Rh(III) porphyrins. Cyclic voltammetric analyses of these porphyrins may thus provide a confirmation of the disproportionation mechanism just proposed.

At 20 °C and 0.1 V/s, the cyclic voltammograms are the same for all three basket-handle porphyrins (of the type shown in Figure 6a for *a*-(di-C₄Ph)₂(CT)RhCl, see also Table 1) as for TPPRh(III)Cl (Figure 2a). The same is true for the UV-vis spectra obtained after thin-layer electrolysis at wave 1 (Table 3). These observations clearly confirm that dimerization does not interfere in the electrochemistry of simple rhodium porphyrins. Both waves 1 and 1' remain irreversible upon raising the scan rate and/or decreasing the temperature for *e*-(C₁₂)₂(CT)RhCl. With *a*-(C₁₂)₂(CT)RhCl, some reversibility appears upon raising the scan rate at -20 °C. This phenomenon appears more clearly for *a*-(di-C₄Ph)₂(CT)RhCl as shown in Figure 6. At -20 °C and 4 V/s, the voltammogram (Figure 6d) consists in two successive reversible one-electron waves (1/1' and 2/2') corresponding to the Rh(III)/Rh(II) and Rh(II)/Rh(I) couples, respectively. The appearance of two waves labeled 2' in Figures 6b and 6c is a reflection of two forms of Rh(I), one nonligated and the other ligated. The fact that the disproportionation

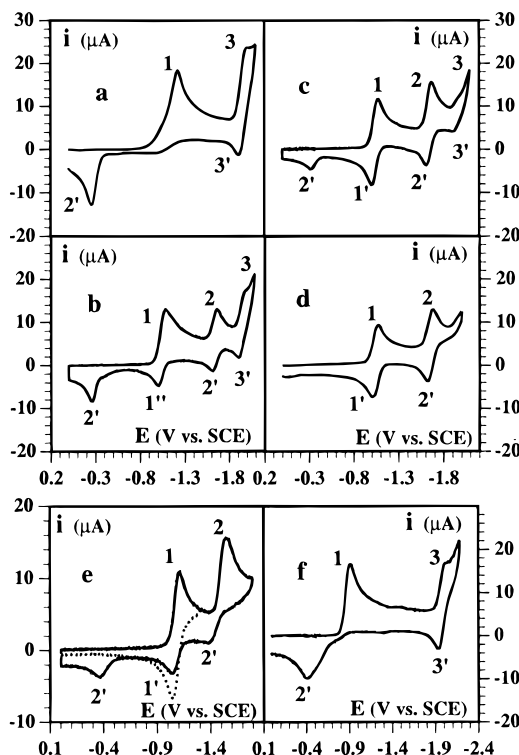


Figure 7. Cyclic voltammograms of TPPRh(I) (1 mM) in *n*-PrCN + 0.1 M Bu₄NClO₄: in the presence of PET₃ ([PET₃] = 0 (a), 1 (b), 3 (c), ≥ 5 (d) mM), of 100 mM PCH₃Ph₂ (e), of 100 mM PPh₃. (f) Scan rate: 0.1 V/s. Temperature: 20 °C.

process is slowed down by the amide-linked structures is caused by a decrease of the deligation rate. The latter effect is likely to result from a stabilization of the negatively charged complexes by the amide dipoles as demonstrated earlier in the electrochemistry of basket-handle iron porphyrins.¹³

Role of Axial Ligands. Tertiary Phosphines. The preceding discussion has emphasized the essential role of ligand exchange reaction in the ECE–disproportionation processes involved in the reduction of Rh(III) into Rh(I) and vice versa. In order to determine if a change in axial ligands may modify or eventually annihilate Rh(II) disproportionation, we have investigated the effect of tertiary phosphines, namely, PET₃, PCH₃Ph₂, and PPh₃, in a weakly ligating solvent, butyronitrile, on the cyclic voltammograms. The most spectacular effect is that of PET₃ (Figure 7). Addition of 5 mM PET₃ totally converts the irreversible 1/2' two-electron wave system (Figure 7a) into two successive one-electron reversible waves, 1/1' and 2/2' (Figure 7d). Further addition neither changes the shapes of the waves nor shifts the peak potentials. This behavior points to the coordination of Rh(III) by two phosphine ligands which remain present upon successive addition of two electrons. At lower PET₃ concentrations (Figures 7b and 7c), the responses are a mixture of the two behaviors. The ECE–disproportionation two-electron reaction is thus totally annihilated as soon as the phosphine concentration reaches 5 mM. It is replaced by the successive addition of two electrons with no loss of ligand, as sketched by the vertical dotted arrows in Scheme 1. We also note in Figure 7d that the reversible wave 3/3' has disappeared, which falls in line with the doubly ligated Rh(I) complex being more oxidizable than the nonligated complex Rh(I) because of the excess of electron density.

This interpretation is confirmed by preparative-scale coulometry (one electron is exchanged reversibly at the potentials of the first and second cyclic voltammetric waves) and by thin-layer spectroelectrochemistry. Figure 8 shows the UV-vis spectra obtained successively at the first and second reduction

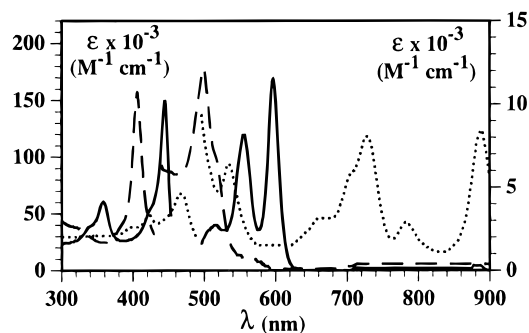


Figure 8. Thin-layer spectroelectrochemistry of TPPRh (0.25 mM) in *n*-PrCN + 0.1 M *n*-Bu₄NClO₄ in the presence of 50 mM PEt₃. Solid line: initial complex. Dotted line: after electrolysis at -1.2 V vs SCE. Dashed line: after further electrolysis at -1.8 V vs SCE.

potentials (see also Table 3). Reoxidation gives back the starting spectrum in each case. The spectrum of the starting Rh(III) has undergone changes indicating that I⁻ has been replaced by PEt₃ as axial ligand. The spectrum obtained after electrolysis at wave 1 is similar to, albeit not identical, the spectrum previously described of a photogenerated TPPRh(II) complex.²³ The small differences observed are likely to be a reflection of the double axial ligation by PEt₃ in the first case as opposed to an absence of axial ligand in the second. The spectrum observed after electrolysis at wave 2 is similar to that of the rhodium(I) complex obtained in the absence of phosphine (Table 3). The bands are red-shifted in accord with a complexation of Rh(I) by two phosphines suggested by the cyclic voltammetric results.

With PCH₃Ph₂ also (Figure 7e), the two-electron irreversible wave leading directly to the Rh(I) complex is replaced by two successive one-electron waves. The first of these is reversible (dotted line in Figure 7e), indicating that the Rh(II) complex bearing two phosphine axial ligands is stable within the time scale of the cyclic voltammetric experiment (0.1 V/s). However, at variance with what was observed with PEt₃, the following wave, 2, is almost completely irreversible, showing that the Rh(I) complex thus formed loses its phosphine ligands. The resulting deligated Rh(I) complex exhibits an oxidation wave on the reverse scan at a much more positive potential, in the same range as in the absence of phosphine. It is interesting to note that a thin-layer spectroelectrochemical experiment at the potential of the first reduction wave does not give rise (Table 3) to the spectrum of the Rh(II) complex but rather to the spectrum of the deligated Rh(I) complex, in apparent contradiction with cyclic voltammetry. This observation shows that deligation of the Rh(II) complex does occur, albeit slowly. It can be observed, together with the ensuing disproportionation reaction, within the time scale of thin-layer spectroelectrochemistry, *ca.* 15 min, but not within the time scale of slow scan cyclic voltammetry, *ca.* 1/4 s at 0.1 V/s.

Addition of PPh₃ does not hamper the occurrence of the ECE-disproportionation process leading directly to the two-electron formation of the Rh(I) complex. Indeed, wave 1 remains irreversible and corresponds to the exchange of two electrons per molecule (Figure 7f). However, the addition of PPh₃ is not without effect on the electrochemistry of rhodium porphyrins. Spectroelectrochemistry shows (Table 3) that the spectrum of the starting Rh(III) has changed reflecting a change in axial ligation. We also note that both wave 1 and wave 2' are shifted in the positive direction.

Appearance of the reversible couples 1/1' and 2/2' upon addition of tertiary phosphines (P(CH₃)₂Ph, PCH₃Ph₂, and PPh₃) and decreasing the temperature has been noted before^{11b} and

can be interpreted by changes in axial coordination in the framework of an ECE-disproportionation mechanism as discussed above. In the original paper, it was rather viewed as resulting from the competition between the formation of a Rh-Rh dimer and of a Rh(III) anion radical.

Conclusions

As shown by cyclic voltammetry, coulometry, and thin-layer spectroelectrochemistry, the electrochemical reduction of rhodium(III) simple porphyrins (TPP, OEP) in usual dipolar aprotic solvents, such as DMSO, DMF, and butyronitrile, is an irreversible two-electron process leading to the corresponding rhodium(I) complex. The reoxidation of the rhodium(I) porphyrin thus obtained takes place at a much more positive potential (by *ca.* 0.5 V). It is also an irreversible two-electron process leading back to the starting rhodium(III) porphyrin. The cause of the irreversibility of rhodium(III) reduction is thus not the metal-metal dimerization of an intermediary rhodium(II) complex as previously believed. This is confirmed by the fact that sterically encumbered porphyrins, such as those bearing cross-trans basket-handle superstructures which forbid the approach of two molecules at bonding distance, exhibit the same behavior as simple rhodium porphyrins. The observed irreversibility in fact derives from a ligand exchange reaction in the coordination sphere of the initially formed rhodium(II) complex which then becomes easier to reduced than the starting rhodium(III) complex. Two electrons are therefore exchanged at the same potential according to an ECE mechanism where the second electron transfer occurs at the electrode surface. Concurrently, the second electron transfer may take place in the solution between the two Rh(II) complexes along a disproportionation pathway.²⁴ This disproportionation of intermediary oxidation states are not frequently encountered in the redox chemistry of metalloporphyrins and related complexes, such as cobalt porphyrins and B12 derivatives. The sluggish oxidation of deligated rhodium(I) porphyrins, which takes place at potentials that are more positive than the reduction of the corresponding rhodium(III) complex, presumably derives from an out-of-plane location of the rhodium atom at the Rh(I) oxidation state resulting in a decrease of the electron density at the rhodium. The tendency of the rhodium atom to stand out of the plane of the porphyrin ring already exists in rhodium(III) complexes.²⁵ It should be enhanced upon injection of additional electrons. It is noteworthy that strong and soft axial ligands may annihilate the ECE-disproportionation process. Typical examples are triethyl- and (dimethylphenyl)phosphines with which two successive one-electron reactions, Rh(III)/Rh(II) followed by Rh(II)/Rh(I), are observed. Rh(III) is then ligated by two phosphines, which remain in the coordination sphere after addition of one and even two electrons. This double axial ligation presumably forces the rhodium atom to remain in the porphyrin plane thus decreasing the reducibility of the rhodium(II) complex.

Experimental Section

Chemicals. The solvents, DMF (Fluka, Burdick & Jackson grade), DMSO (Fluka, Burdick & Jackson grade), and butyronitrile (Fluka purum >99%), were used as received. The supporting electrolytes, Et₄NClO₄ and *n*-Bu₄NClO₄, were recrystallized (three times in a 2:1 ethanol-ethyl acetate mixture for the former and one time in a 2:1 acetone-water mixture for the latter) and vacuum dried at 50 °C before use. Triphenylphosphine (Fluka puriss), methylphenylphosphine (Aldrich, 99%), and triethylphosphine (Strem 99%) were used without further purification.

(24) This conclusion falls in line with the observation that the dimer of OEPRh(II) disproportionates upon dissolution in pyridine.^{9d}

(25) Bärnighausen, H.; Handa, B. K. *J. Less-Common Metals* **1964**, *6*, 226.

(23) Hoshino, M.; Yasufuku, K.; Konishi, S.; Imamura, M. *Inorg. Chem.* **1984**, *23*, 1982.

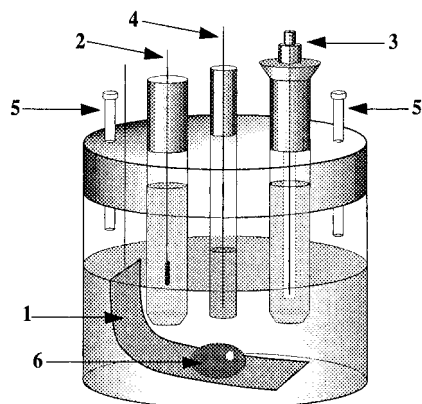


Figure 9. Cell for preparative-scale electrolysis. (1) Carbon felt working electrode. (2) Pt wire counterelectrode with glass frit separator. (3) NaCl-saturated calomel reference electrode. (4) Glassy carbon disk electrode for in situ cyclic voltammetric control. (5) Septum for solution sampling. (6) Magnetic stirrer.

TPPH₂ was purchased from Aldrich. OEPH₂^{26a} and the free bases of the basket-handle porphyrins were prepared as described earlier.^{26b,c} For the other porphyrins, rhodium was inserted as described below.

(a) TPPRhNH(CH₃)₂Cl. A mixture of 0.24 mM TPPH₂ and 0.95 mM RhCl₃ in 200 mL of DMF is refluxed overnight under argon. After vacuum evaporation of the DMF at room temperature, the solid phase is dissolved in CH₂Cl₂, washed three times in distilled water, dried over anhydrous Na₂SO₄, filtrated, and evaporated. Silica gel thin-layer chromatography reveals the presence of two products, which are separated by chromatography on a silica gel column eluted successively with CH₂Cl₂ and a 3:1 CH₂Cl₂–(C₂H₅)₂O mixture yielding the free base and the rhodium porphyrin successively. The latter is purified by preparative silica gel thin-layer chromatography with 7.5:1 CH₂Cl₂–(C₂H₅)₂O elution. The solid phase is then washed with a 1:1 methylene chloride–acetone mixture and recrystallized from CH₂Cl₂ and hexane. The overall yield is 30%. ¹H NMR (CDCl₃, 200 MHz) δ (ppm): 8.90 (s, 8H, H pyr), 8.32 (m, 4H, H phe o), 8.16 (m, 4H, H phe o'), 7.7 (m, 12H, H phe m et p), –3.24 (m, 4H, H (CH₃)₂NH). UV-vis (CH₂Cl₂) λ (nm) (ϵ L mmol^{–1} cm^{–1}): 426 (259.4), 537 (25.5), 570 (6.0). Anal. Calcd for C₄₄H₃₅N₅ClRh·0.5 H₂O: C, 68.62; H, 4.51; N, 8.70. Found: C, 68.50; H, 4.45; N, 8.38.

(b) TPPRhCl. A mixture of 0.7 mM TPPH₂ and 0.77 mM [Rh(CO)₂Cl]₂ in 150 mL of toluene is refluxed overnight under argon. After vacuum evaporation of the toluene at room temperature, the solid phase is dissolved in toluene and CH₂Cl₂. Chromatography on a silica gel column eluted successively with toluene, CH₂Cl₂, and a 1:1 methylene chloride–acetone mixture yields successively TPPRh₂(CO)₄ and two fractions containing Rh(III). The latter are purified by preparative silica gel thin-layer chromatography with CH₂Cl₂ elution. The solid phase is then washed successively with a 1:1 methylene chloride–acetone mixture and a 10:1 methylene chloride–methanol mixture and recrystallized from CH₂Cl₂ and hexane. The overall yield is 31.5%. ¹H NMR (CDCl₃, 200 MHz) δ (ppm): 8.92 (s, 8H, H pyr), 8.22 (m, 8H, H phe o et o'), 7.77–7.74 (m, 12H, H phe m et p). UV-vis (CH₂Cl₂) λ (nm) (ϵ L mmol^{–1} cm^{–1}): 422 (200.6), 534 (19.1), 566 (3.5). Anal. Calcd for C₄₄H₂₈N₄ClRh·2H₂O: C, 67.14; H, 4.10; N, 7.12. Found: C, 67.47; H, 4.54; N, 6.26.

(c) TPPRhI. An argon-deaerated solution of 0.24 mM [Rh(CO)₂Cl]₂ in 15 mL of CHCl₃ is added dropwise to 0.16 mM TPPH₂ in the same solvent. The resulting mixture is left overnight under agitation. It is then oxidized by I₂ in two successive additions: 0.16 mM, and after 2

h, 0.08 mM. The solution is left for 5 h under agitation. After filtration and evaporation, the solid phase is dissolved in CHCl₃. Chromatography on an alumina column eluted with CHCl₃ yields successively TPPRh₂(CO)₄ and TPPRhI. The latter is recrystallized from CHCl₃ and hexane. The overall yield is 40–60%. ¹H NMR (CDCl₃, 200 MHz) δ (ppm): 8.22 (m, 8H, H phe o et o'), 7.76 (m, 12H, H phe m et p). UV-vis (CH₂Cl₂) λ (nm) (ϵ L mmol^{–1} cm^{–1}): 424 (177.7), 534 (19.7), 566 (3.7). Anal. Calcd for C₄₄H₂₈N₄IRh·H₂O: C, 61.41; H, 3.51; N, 6.51. Found: C, 61.77; H, 3.83; N, 6.15.

(d) OEPRhCl. OEPH₂ (0.37 mM) and [Rh(CO)₂Cl]₂ (0.45 mM) in 190 mL of toluene are reacted overnight under argon at room temperature. After evaporation of the toluene, the solid phase is purified by chromatography on a silica gel column eluted successively with toluene and a 3:1 toluene–acetone mixture. A second purification is carried out by preparative silica gel thin-layer chromatography with 10:1 toluene–acetone elution. The solid phase is then washed several times with a 1:1 toluene–acetone mixture and a 10:1 toluene–methanol mixture and finally recrystallized from CH₂Cl₂ and hexane. The overall yield is 15.5%. ¹H NMR (CDCl₃, 200 MHz) δ (ppm): 8.01 (t, 24H, CH₂CH₃), 5.85 (q, 16H, CH₂CH₃), 0.31 (s, 4H, CH=). UV-vis (CH₂Cl₂) λ (nm) (ϵ L mmol^{–1} cm^{–1}): 401 (127.3), 520 (11.5), 552 (23.3). Anal. Calcd for C₃₆H₄₄N₄ClRh: C, 64.43; H, 6.56; N, 8.35. Found: C, 64.38; H, 6.64; N, 8.32.

(e) a-(C₁₂)₂(CT)RhCl. A solution of 0.38 mM [Rh(CO)₂Cl]₂ in 20 mL of DMF is added dropwise to 0.14 mM of the free base dissolved in 50 mL of DMF at a temperature of 160 °C. The mixture is then refluxed under argon for 48 h. After vacuum evaporation of the DMF at room temperature, the solid phase is dissolved in CH₂Cl₂, washed three times with water, dried over anhydrous Na₂SO₄, filtrated, and evaporated. After dissolution in CH₂Cl₂, chromatography on a silica gel column eluted successively with a 1:1 CH₂Cl₂–(C₂H₅)₂O mixture and a 1:1 methylene chloride–acetone mixture yields two fractions, the free base and the rhodium porphyrin. The latter is purified by preparative silica gel thin-layer chromatography with 5:1 methylene chloride–acetone elution. The solid phase is then washed with a 1:1 methylene chloride–acetone mixture and recrystallized from CH₂Cl₂ and hexane. The overall yield is 13.1%. ¹H NMR (CDCl₃, 200 MHz) δ (ppm): 8.85 (s, 8H, H pyr), 8.8–7.5 (m, 16 H, H phe), 6.3 (m, 2H, H amide), 3.9–0.0 (40H, H CH₂). UV-vis (CH₂Cl₂) λ (nm) (ϵ L mmol^{–1} cm^{–1}): 430 (95.2), 539 (13.2), 572 (5.2).

The same procedure is used for a-(diC₄Ph)₂(CT)RhCl (overall yield: 9.8%. UV-vis (CH₂Cl₂) λ (nm) (ϵ L mmol^{–1} cm^{–1}): 431 (123.5), 540 (11.5), 552 (23.3)) and e-(C₁₂)₂(CT)RhCl (¹H NMR (CDCl₃, 200 MHz) δ (ppm): 8.8 (s, 8H, H pyr), 8.2–7. (m, 18H, H ph), 3.9 (m, 8H, Ha CH₂), 0.9 (m, 8H, Hb CH₂), 0.0–0.8 (m, 32 H, Hg-h CH₂). UV-vis (CH₂Cl₂) λ (nm) (ϵ L mmol^{–1} cm^{–1}): 428 (163.2), 538 (17.9), 570 (3.8)).

Instrumentation. Cyclic voltammetry experiments are carried out in a thermostated three-electrode cell. The working electrode is a 3 mm diameter glassy carbon (Tokai) rod sealed with epoxy in a glass tube. The disk exposed to the solution is frequently polished with 15-to-1 μ m diamond pastes. The counter electrode is a platinum wire, and the reference electrode a saturated NaCl calomel electrode (in all of the cyclic voltammograms above, the potential axis has been corrected so as to be referenced to the usual SCE electrode). The instrument is composed of a function generator (PAR 175), an x–y recorder (IFFELEC 2502), and a home-built potentiostat and current measurer equipped with positive feedback resistance compensator.²⁷

The cell (6 cm³) used for preparative-scale electrolysis is sketched in Figure 9. This set-up allows the recording of cyclic voltammograms at any moment during electrolysis. All electrolyses were carried out in a water and oxygen-free glovebox.

The thin-layer UV-vis spectroelectrochemical set-up is the same as previously described.^{14a} A platinum grid electrode was used as the working electrode.

(26) (a) Sessler, J. L.; Mozaffari, A.; Johnson, M. R. *Org. Synth.* **1991**, 70, 68. (b) Momenteau, M.; Mispelter, J.; Loock, B.; Lhoste, J.-M. *J. Chem. Soc., Perkin Trans. 1* **1985**, 221. (c) Momenteau, M.; Mispelter, J.; Loock, B.; Bisagni, E. *J. Chem. Soc., Perkin Trans. 1* **1983**, 189.

(27) Garreau, D.; Savéant, J.-M. *J. Electroanal. Chem.* **1972**, 35, 309.